Next-Generation-Sequencing Data for Mouse Models: Applications and analysis in context of a pre-clinical oncology drug development

by Hagen Klett
and Julia Schueler

Next-generation sequencing (NGS) capabilities have evolved in recent years with significant improvements in robustness, data interpretation, time lines, and costs. The integration of these technologies into the drug development process has markedly changed the preclinical and clinical landscape, specifically (but not exclusively) in oncology research. The possibility to create large datasets across a broad range of cancer types provides deep insights into the genomic landscape of cancer and enables the identification of new potential therapeutic targets.[1] An understanding of the functionality of these alterations and the influence they have on treatment response, however, relies on the availability of predictive and robust preclinical models reflecting the clinical landscape.[2]

Preclinical studies in oncology are frequently based on the use of mouse models. On average, the protein-coding regions of mouse and human genomes are 85% identical and the mouse genome can be easily manipulated. A notable difference, however, is that the genomic identity between H. sapiens and M. musculus cannot compensate for significant species differences influencing the outcome of experiments investigating specific aspects of tumor biology or anticancer drug activity.

Timeline for Development of PDX Mouse Models

Rodent tumor models have been generated since the 1960s, with xenografts of human tumor models emerging in the 1980s.[3] The development of the nu/nu mutant mouse lacking functional thymus tissue and therefore T cells enabled the engraftment and serial transplantation of human tumor tissue into mice.[4] With the development of more immunosuppressive mouse strains like SCID, NOD/SCID or most recently NOD/SCID/IL2Rγnull (NOG and NSG) mice the engraftment rate of human tumor tissue

improved significantly over the last 30 years. Notably the latter enabled not only an improved engraftment of solid tumors but the establishment of PDX from hematological malignancies, namely, acute leukemia and different types of lymphomas.[5,6]

Pioneer studies conducted in the 1980s already showed a high degree of correlation between clinical response and corresponding PDX sensitivity towards cytotoxic agents in Non-small cell lung cancer and childhood rhabdomyosarcomas.[7,8] In addition, PDX models have been used to conduct preclinical phase II studies with classic chemotherapeutics.[3]

In more recent times, there have been multiple efforts in industry as well as academia to establish large panels of well-characterized patient-derived xenograft (PDX) models covering a wide range of different tumor types. Indeed, these collections are becoming the preferred research tool to optimize the drug development process at multiple steps, in particular for target validation, pharmacology and translational studies.[9-12] Currently, these collections represent the preclinical oncology platform most consistently displaying the complexity of tumor heterogeneity and molecular diversity of human cancers

In this study, we present a potential workflow for the investigation of novel anti-cancer molecules using the example of EGFR targeting small molecules as well as antibodies evaluated on the PDX *in vitro* and *in vivo* preclinical platforms.

Comparative datasets generated on various assay platforms for PDX mouse models

The Charles River Tumor Model Compendium was used as a database for tumor model selection for subsequent drug testing of different EGRF inhibitors. At present, the tumor model collection comprises 751 tumor models in total; 459 of them are available as PDX models (**Figure 1**). The collection covers all important entities ranging from widespread diseases like colon, lung or breast cancer to rare diseases like ovarian or thyroid cancer. Tumor models were chosen based on EGFR expression of Affymetrix HGU133plus2.0 microarray and RNA-seq data (see Materials and Methods for details).

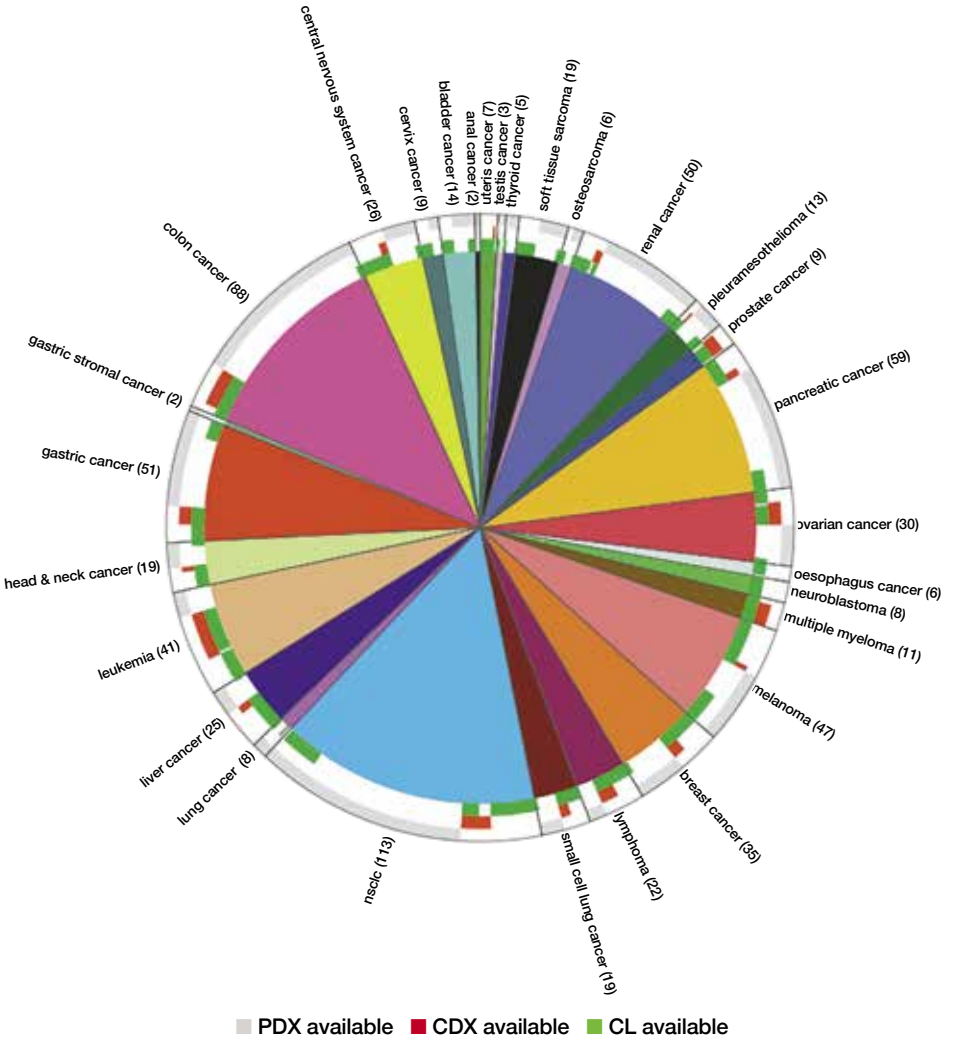

Figure 1: Panel of available PDX tumor models in the Charles River Tumor Model Compendium as of January 2019.

Gene expression correlation of the models: EGFR expression was mutually corroborative (Pearson's correlation coefficient = 0.85) between the two different gene expression platforms suggesting both as confident sources for model selection. Thus, both platforms were used to select potential responders or non-responders to targeted therapy against EGFR (see **Figure 2**).

Target protein expression correlation of the models: For further confirmation of target expression on the protein level, an immunohistochemistry (IHC) to detect EGFR surface protein was performed on the complete PDX panel. To streamline this screening approach a tissue micro array (TMA) was created including all PDX models in duplicates. The IHC results were quantified using an inhouse software solution (OSANO) (for details see Materials and Methods). The protein expression level measured as DAB+ area correlated significantly with the RNA expression level (**Figure 3**, Student's t-test: p-value <0.05). Based on RNA as well as protein expression levels, we selected high expression models as well as low expressers. The latter serving as negative controls for the subsequent drug screening. In all, 13 EGFR inhibitors (EGFRi) were tested in a 2D assay in 96-well format on 74 PDX derived cell lines (for details

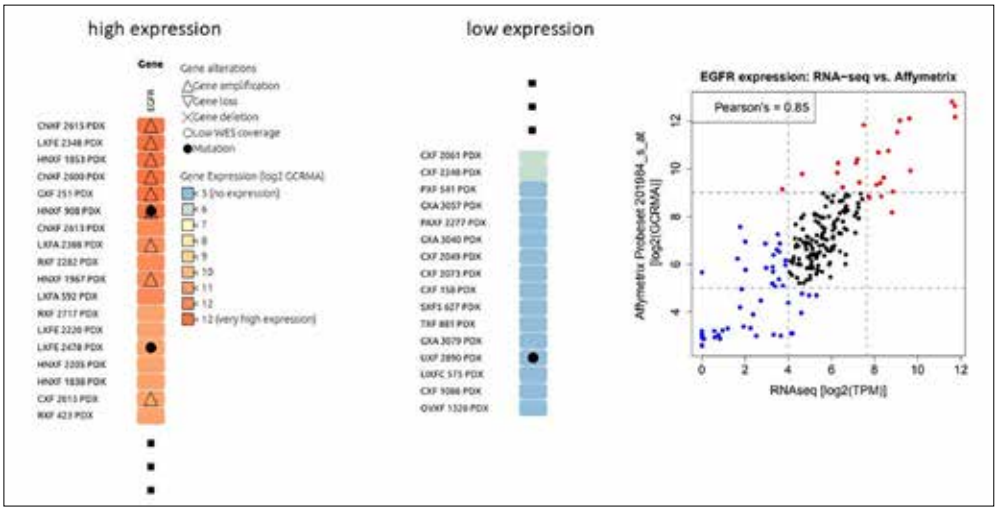

Figure 2: Correlation between gene expression microarray and RNA-seq data. Blue and red points indicate low (Affymetrix HGUI33p2 log2(gcRMA) <5 or RNA-seq TPM <20) and high (Affymetrix HGUI33p2 log2(gcRMA) >10 or RNA-seq TPM >200) EGFR expressing models, respectively.

see Materials and Methods).

Activity testing of the models with drugs: Specific anti-proliferative activity was determined for the small molecules Afatinib, Erlotinib, Gefitinib and Lapatinib. For those compounds the IC50 was significantly lower in EGFR high expressing models compared to low expressing lines (Student's t-test: p-value <0.05). The cut-off for high vs low expression was defined as ≥25 vs <25 protein abundance, respectively (**Figure 4**). Subsequently, a total of 296 PDX models including the 74 of the 2D screen were utilized to test the ten most active EGFRi in an *ex vivo* 3D screen. For the Image Analysis (IA) 3D assay, selective sensitivity towards Erlotinib was observed for models with high EGFR protein abundance, confirming the 2D assay. This effect could not be detected for Afatinib, Gefitinib or Lapatinib.

Metabolic assays: A metabolic read-out (cell titer glow™, CTG) based on the same 3D assay confirmed the previous results: models with high EGFR protein abundance showed higher sensitivity against the small molecule Erlotinib.

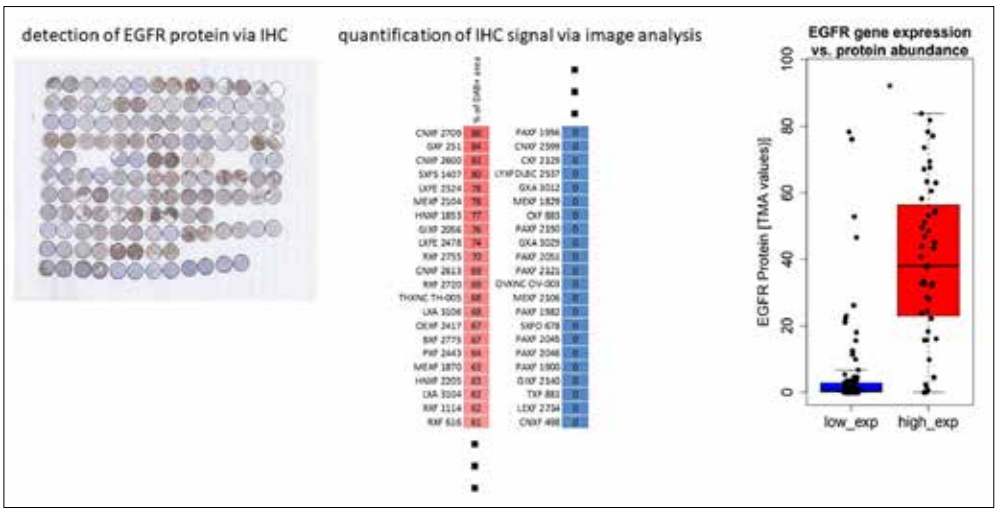

Figure 3: EGFR expression was confirmed by IHC on tissue micro arrays (TMAs) of the complete PDX panel. TMAs were quantified using the OSANO software giving a relative measure of protein abundance. High EGFR gene expressers showed a significantly higher EGFR protein abundance than low expressers (Student's t-test: p-value <0.05).

For subsequent analyses and testing, sensitive models were defined as IC50 <½ geometric mean, while the remaining models were labeled resistant. By combining the results of the 3D assays with the 2D screen, we thereby obtained an extended list of sensitive and resistant models.

In vivo testing: Seven EGFRi agents were tested *in vivo* in 174 different subcutaneously implanted PDX models using five small molecules (Axitinib, Cetuximab, Erlotinib, Necitumumab, Sorafenib and Sunitinib) and two antibodies (see **Figure 5** and **Table 1**). As a value for general sensitivity towards EGFR inhibition the mean optimal tumor growth inhibition ratio (T/C value) was calculated for each model across all tested compounds. These mean optimal T/C values were compared between models with high EGFR protein abundance and those with low protein abundance (cut-off defined as 33).

The high expressing models depicted a significantly lower mean optimal T/C value than those with low target expression (Student's t-test p-value <0.05): 33.86±14.4% in the EGFR high expresser group (33 models) and 57.61±12.1% in the EGFR low expresser group (136 models). Thus, EGFR target expression discriminated the sensitive and resistant models in a statistically significant manner. As Erlotinib showed a selective anti-proliferative activity most consistently across different platforms (2D vs 3D) and read-outs (IA vs CTG) a correlation analysis between *in vivo* and *in vitro* data was performed: Ten sensitive and 28 resistant PDX models were selected based on *in vitro* data and the optimal T/C values of the *in vivo* studies analyzed.

Indeed, the median optimal T/C value of the predicted sensitive models was statistically significant lower as the median optimal T/C value of the PDX panel predicted to be resistant (Student's t-test p-value <0.05). Proceeding from those results, we identified in vivo responders (T/C value <30th percentile) and non-responders (T/C value >30th percentile) for Erlotinib in the PDX panel consisting of 38

models. Automated and adapted bioinformatic analyses were applied to establish a predictive biomarker signature for Erlotinib. Molecular data, including mutation data (whole exome sequencing), expression (HGUI33v2 microarray and RNA-seq), and copy number data (Snp6) as well as model-related meta-data build the foundation of the analysis (**Figure 6**).

In our investigation of the meta-data of the treated PDX models, we observed significant lower median doubling times for responders (p-value <0.05), indicating a potential selection criteria for future drug development studies. Hierarchical clustering of the top 30 differentially expressed genes showed a clear separation between responders and non-responders with two responders clustering within the non-responsive group and one non-responder within the responsive group. Corroborating the results from the *in vitro* and *in vivo* experiments, there was EGFR itself as well as genes associated with EGFR signaling, cell proliferation, ERBB2 signaling and chemokine induction among the top 30 differentially expressed genes between the responder and the non-responder group (analysis was performed with https://www.pathwaycommons.org/).

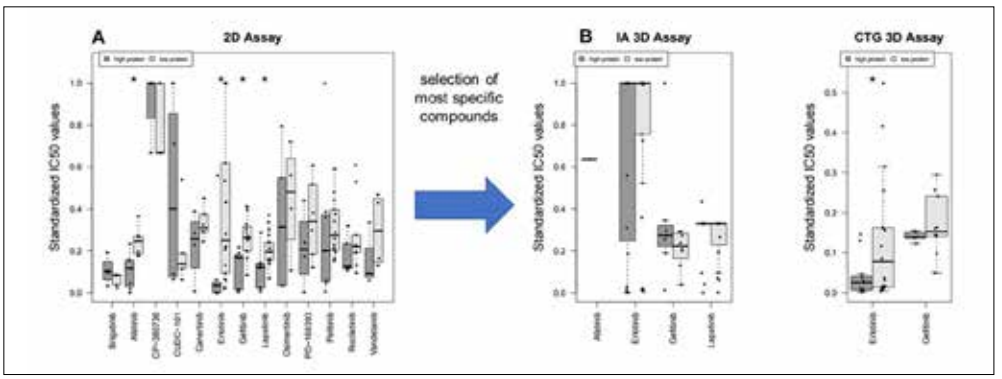

Figure 4: IC50 values were collected in 2D (A) and 3D (B) of 13 EGFRi in 74 PDX derived cell lines. Data is shown for models that were selected based on gene expression values. IC50 values are shown according to their EGFR protein abundance (high ≥25 and low <25). * indicates significant differences (Student's t-test: p-value <0.05).

Discussion

In the current study detailing the well-known target EGFR, we show that the drug development process benefits from NGS data at every step – from target ID throughout pharmacology and biomarker development. The combination of genomic and phenotypic screening enhanced the efficiency and efficacy of the drug development process specifically at the target discovery and validation, *in vitro*/*in vivo* pharmacology and biomarker development.

The recent advent of NGS data availability in the pre-clinical space has made it possible to integrate genome-, proteome-, and phenotype-based drug screening methods in the precision medicine paradigm. While the use of PDX models (versus conventional cell line-based models) add an additional layer of complexity to the study, these models better reflect intra-tumoral heterogeneity of the donor patient tissue.[13] These trade-offs need to be taken into account when considering NGS techniques applied to PDX materials.

It might be necessary to use material from different donor mice and/or different passages specifically for expression data to get a representative data set of the PDX model. A caveat here is that the cells to be analyzed from xenograft or PDX tissue may contain chimeric material (human tumor cells surrounded by murine cells) in the tumor microenvironment. A number of different pipelines is described to decode mouse from human signals with the aim to improve the accuracy of the molecular data.[14-17]

Despite those hurdles, establishment, characterization, and validation of PDX models has been ongoing for decades, especially in oncology drug development and tumor biology research. As the value of PDX models become more evident,[18-20] they will join genetically engineered mouse models and cell line derived xenografts as a complementary option in preclinical oncology studies. Bearing in mind the above-mentioned caveats related to molecular analyses of PDX material, multiple initiatives in academia (e.g., EuroPDX and PDXfinder) as well as industry (e.g., Repositive) are under way to build such tools for applications.

A database of PDX-related research has the potential to enhance the translational impact of PDX in general. Harmonized annotation of the models and comprehensive molecular profiling including genomics and proteomics platforms are key features to the success of such approaches.[10] In this paper, we have shown the potential of NGS data of PDX and other preclinical models as useful assets in the drug development process in a targeted as well as a phenotypic approach. The combination of NGS with proteomics and image analysis data will further elucidate the predictivity of the preclinical models and enhance their translational impact.

Material & Methods

PDX establishment

This study was carried out in strict accordance with the recommendations in the Guide for the Care and Use of Laboratory Animals of the Society of Laboratory Animals (GV SOLAS). All animal experiments were approved by the Committee on the Ethics of Animal Experiments of the regional council (Permit Numbers: G-09/58, G-13/13 and G13/43). 4-6 week old female NMRI nu/nu mice (Charles River, Germany) placed under isoflurane anesthesia received tumor implants subcutaneously in both flanks. During the first passages, mice were monitored for tumor growth for up to 12 months. When stable tumor growth could be determined, mice were sacrificed and tumor material was implanted into new recipient mice. In addition, xenograft

material was stored in liquid nitrogen for future implantation or fixed in formalin and stored liquid nitrogen for subsequent analyses. A PDX was defined as established when stable growth over at least 3 passages and regrowth from liquid nitrogen could be observed. The percentage of tumor implants displaying stable growth (take rate) and passage time were recorded for every model and every individual passage. Tumor growth was determined by a two-dimensional measurement with calipers weekly or biweekly depending on the growth characteristics of the respective PDX model. Tumor volumes were calculated according to the following equation: Tumor Vol [mm3] = a [mm] x b2 [mm2] x 0.5, where "a" is the largest diameter and "b" is the perpendicular diameter of the tumor representing an idealized ellipsoid. Animals had to be sacrificed when tumor volume reached 1.800 mm3.

Table 1: *In vivo* Dosing scheme for different EGFR inhibitors

Compound	Dose [mg/kg/d]	Schedule [d]	Application route
Axitinib	25	0-31	Orally
Cetuximab	30	0,7,14	Intraperitoneally
Erlotinib	50	0-21	Orally
Necitumumab	20	Twice weekly	Intraperitoneally
Pazopanib	100	0-14	Orally
Sorafenib	200	0-4	Orally
Sunitinib	40	0-31	Orally

Treatment experiments *in vivo*

Implantation was performed similar to PDX establishment, except that animals received bilateral tumor implants. Animals and tumor implants were monitored daily until the maximum number of implants showed clear signs of beginning solid tumor growth. At randomization, the volume of growing tumors was initially determined. Animals bearing 50-250mm3 tumors, preferably 80-200mm3, were distributed into experimental groups, with comparable median and mean tumor volumes. The day of randomization was designated as day 0 of an experiment and was also the first day of dosing. All compounds were applied via common application routes according to the relevant animal welfare guidelines published by FELASA and GV-SOLAS. Tumor volume and body weight were determined twice weekly.

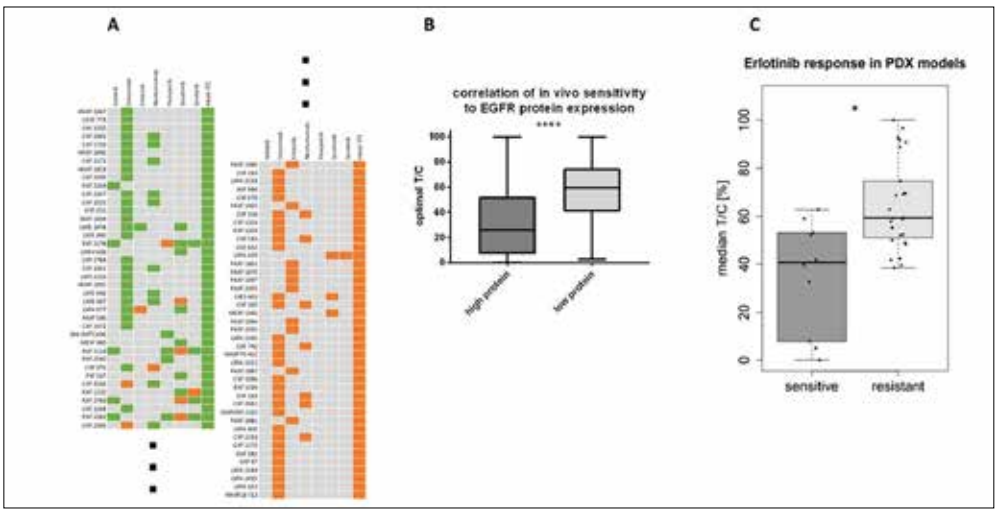

Figure 5: (A) seven EGFRi were tested in 169 subcutaneously implanted PDX models *in vivo*. T/C values were determined as described in M&M. The mean optimal TC/ value was calculated for each model across all tested compounds. (B) For models with measured EGFR protein abundance, median optimal T/C values of models with EGFR high (≥25) protein abundance was compared to those with low protein abundance (<25). **** indicates significant differences (Student's t-test: p-value <0.0001). (C) The anti-proliferative activity of Erlotinib was compared in sensitive vs resistant PDX models. The classification of the PDX models was performed based on in vitro 2D and 3D data. The box plot showed the differences of T/C values with respect to in vitro sensitivity. * indicates significance (Student's t-test p-value <0.05)

Evaluation of anti-tumoral activity

The relative volume of an individual tumor on day X (RTVx) was calculated by dividing the absolute volume [mm3] of the respective tumor on day X (Tx) by the absolute volume of the same tumor on the day of randomization, i.e., on day 0 (T0), multiplied by 100, as shown by the following equation:

$$Tx/T0*100 = RTVx$$

RTVs were used for compound activity rating as follows: ≤10 = complete remission; >10 ≤50 = partial remission; >50 ≤75 = minor remission; >75 ≤125 = no change; >125 progression. Tumor inhibition on a particular day (T/Cx) was calculated from the median RTV of a test group and the median RTV of a control group multiplied by 100, as shown by the following equation:

$$=xT/C\ [\%] \text{ median RTV treated group}$$
$$\text{medianTRV control group } 100x\ x\ x$$

The minimum T/C [%] value recorded for a particular group during an experiment represented the maximum anti-tumor activity for the respective compound.

FFPE samples, TMA and IHC

FFPE: Tumors were collected immediately after euthanasia of the donor animal. FFPE fixation was performed in 10% neutral buffered formalin for 24 hours followed by routine processing and embedding into paraffin

TMA: Whole tumor sections (4µm) were cut and stained with Hematoxylin-Eosin (H&E). H&E sections of the xenografts were studied by light microscopy and representative areas marked on the slides. Xenograft biopsies, lmm in diameter, were taken from the corresponding area in the paraffin block and arrayed in duplicates into a new recipient block as described.

EGFR IHC: After antigen retrieval, 5M FFPE tissue sections were incubated with anti-human EGFR Antibody (1:36; Dako Cat# M7239, Lot 20055023) overnight at 4°C, followed by DAB staining and hematoxylin counterstaining. Image analysis Digitalized images of the IHC slides were evaluated to determine the percentage of EGFR positive areas using OSANO software. A computerized analysis for digitized whole-slide images of the samples was used to quantify the EGFR expression using color classification and morphological image processing techniques.

Mutational analysis (Whole exome sequencing)

Mutation analysis was performed by whole exome sequencing (Agilent kitsV1 38MB, V4 51MB, V5 50MB or V6 60MB) and utilizing the Ilumina HiSeq-2000/2500/4000 sequencers in 100bp, 126bp and 150bp paired-end reads and an expected coverage on targets of ~100X. Next, mouse stroma was discarded and mutations were called following the GATK best practice pipeline. Candidate mutations were annotated and filtered considering only variants with moderate or high protein impact and those being rare in healthy populations (<5% in dbSNP).

Affymetrix HGU133plus2

Gene expression profiles were obtained by Affymetrix HGUl33plus2 microarray chips and subjected to stringent quality control measures. Expression values extracted from .CEL files and calculated and log 2 transformed using R/Bioconductor packages (gcRMA).

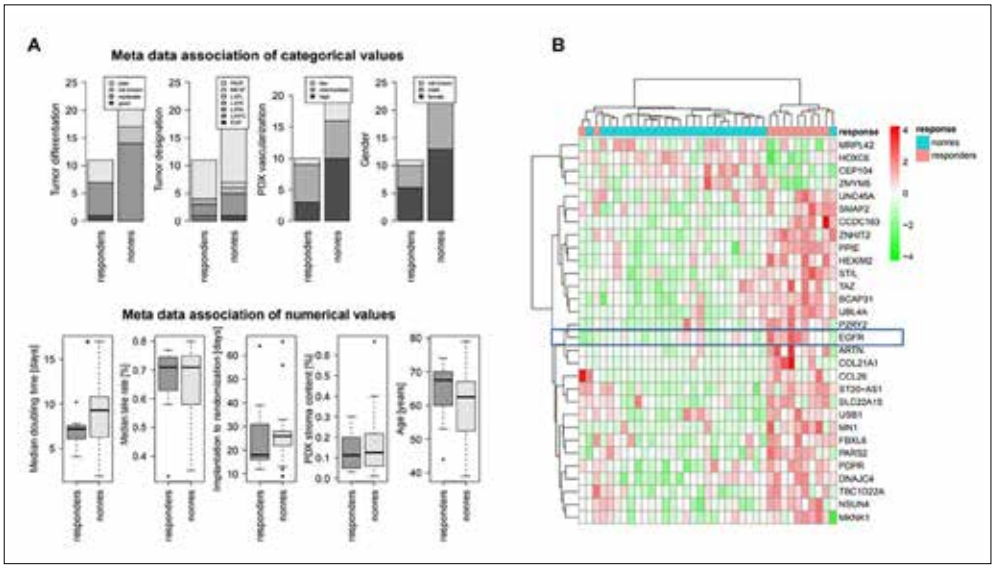

Figure 6: (A) Student's t-test was utilized for numerical covariates and Fisher's exact test for categorical covariates. Significant lower median doubling times were observed for responders (p-value <0.05), indicating a potential selection criteria for therapy. (B) Hierarchical clustering of top 30 differentially expressed genes between responders and non-responders. Responders are associated, inter alia, with high EGFR expression (blue box).

RNAseq

Total RNA was digested by DnaseI (NEB) and purified by oligo-dT beads (Dynabeads mRNA purification kit, Invitrogen). then poly(A)-containing mRNA were fragmented into 200-250bp with Fragment buffer (Ambion). Sequencing was done using IlluminaHiSeq-2000/2500/4000in 100/126bp paired-end (PE) reads with an expected throughput of 10G bases per sample. Next, mouse stroma was discarded and reads were utilized to obtain gene expression (using tophat2 and cufflinks), to call mRNA mutations (following the GATK best practice pipeline), to identify fusion genes (using fusioncatcher), and to decipher the HLA-type (using seq2HLA).

Statistical analysis

For the evaluation of the statistical significance of antitumor efficacy, the non-parametric Kruskal-Wallis test followed by Dunn's method for pairwise comparisons were performed. Individual RTVs of test and control groups were compared on days on which the minimum T/C values were achieved in the test groups. For statistical analysis of survival data, the Log-rank (Mantel-Cox) test was applied. For the evaluation of the statistical significance in all other cases, the Mann-Whitney test (two-tailed) was used unless otherwise indicated. By convention, p-values ≤0.05 indicate significant differences. Statistical calculations were performed using GraphPad Prism bio-analytic software (version 6.02 for Windows, GraphPad Software, San Diego California USA, www.graphpad.com).

Cell culture experiments

Cell line establishment Single cell suspensions from tumor tissue from established PDX were prepared and cells were cultured in RPMI 1640 medium 2ed with 10% (vol/ vol) fetal bovine serum, 1% (vol/vol) Gentamycin and 1% (vol/vol) L-glutamine (all from GIBCO-BRL, Grand Island, NY, USA). Cells were maintained at 37°C and 5% CO_2. Cells were kept in serial passage until all mouse cells were depleted and a stable line was established (passage number 20). A STR-analysis was performed to confirm human origin and to prove conformity with the donor PDX.

2D assay

A modified propidium iodide assay was used to assess the effects of lscador extracts on the growth of the human tumor cell lines.

Briefly, cells were harvested from exponential phase cultures by trypsinization counted and plated in 96-well flatbottomed microtiter plates at a cell density depen dent on the cell line (5-12,000 viable cells/well). After 24h recovery to allow the cells to resume exponential growth, 10µl of culture medium (six control wells per plate) or culture medium containing the respective compound was added to the wells. Following 4 days of continuous drug exposure, cell culture medium with or without drug was replaced by 200 ltl of an aqueous propidium iodide (PI) solution (7µg/ml). The fluorescence was measured using the Cytofluor 4000 microplate reader (excitation 530nm/emission 620nm), giving a direct relationship to the total cell number.

3D assay

A modification of the clonogenic assay as described by Hamburger and Salmon was used.[21] The bottom layer consisted of 0.2ml/well, Iscove's modified Dulbecco medium supplemented with l-glutamine (Life Technologies), 20% fetal calf serum and 0.75% agar; cells were added to 0.2ml of the same culture medium containing 0.4% (w/v) agar and plated in 24-multiwell dishes on top of the bottom layer. Test substances were added (drug overlay) in 0.2ml culture medium under continuous exposure. Every dish included six untreated control wells and drug-treated groups in triplicate. Cultures were incubated at 37°C under 7.5% CO_2 in a humidified atmosphere for up to 25 days and monitored closely for colony growth using an inverted microscope. Within this period, in vitro tumour growth led to the formation of colonies of >50 mm diameter. At the time of maximum colony formation, vital colonies were stained with a sterile aqueous solution of 2-(4-iodophenyl)-3-(4-nitrophenyl)-5-phenyltetrazolium chloride (1 mg/ml, 100ml/well) for 24h. Colony counts were then done with an automatic image-analysis system (OMNICON 3600; Biosys GmbH). ■

References

1. Kamps R, Brandao RD, Bosch BJ, Paulussen AD, Xanthoulea S, Blok MJ, et al. Next-Generation Sequencing in Oncology: Genetic Diagnosis, Risk Prediction and Cancer Classification. International journal of molecular sciences. 2017;18(2). Epub 2017/02/02. doi: 10.3390/ijms18020308. PubMed PMID: 28146134; PubMed Central PMCID: PMCPMC5343844.
2. Kawaguchi T, Foster BA, Young J, Takabe K. Current Update of Patient-Derived Xenograft Model for Translational Breast Cancer Research. Journal of mammary gland biology and neoplasia. 2017;22(2):131-9. Epub 2017/04/30. doi: 10.1007/s10911-017-9378-7. PubMed PMID: 28451789; PubMed Central PMCID: PMCPMC5511343.
3. Boven E, Winograd B, Berger DP, Dumont MP, Braakhuis BJ, Fodstad O, et al. Phase II preclinical drug screening in human tumor xenografts: a first European multicenter collaborative study. Cancer research. 1992;52(21):5940-7. Epub 1992/11/01. PubMed PMID: 1394220.
4. Pantelouris EM. Absence of thymus in a mouse mutant. Nature. 1968;217(5126):370-1. Epub 1968/01/27. PubMed PMID: 5639157.
5. Sugimoto K, Hayakawa F, Shimada S, Morishita T, Shimada K, Katakai T, et al. Discovery of a drug targeting microenvironmental support for lymphoma cells by screening using patient-derived xenograft cells. Scientific reports. 2015;5:13054. Epub 2015/08/19. doi: 10.1038/srep13054. PubMed PMID: 26278963; PubMed Central PMCID: PMCPMC4538400.
6. Vick B, Rothenberg M, Sandhofer N, Carlet M, Finkenzeller C, Krupka C, et al. An advanced preclinical mouse model for acute myeloid leukemia using patients' cells of various genetic subgroups and in vivo bioluminescence imaging. PloS one. 2015;10(3):e0120925. Epub 2015/03/21. doi: 10.1371/journal.pone.0120925. PubMed PMID: 25793878; PubMed Central PMCID: PMCPMC4368518.
7. Fiebig HH, Neumann HA, Henss H, Koch H, Kaiser D, Arnold H. Development of three human small cell lung cancer models in nude mice. Recent results in cancer research Fortschritte der Krebsforschung Progres dans les recherches sur le cancer. 1985;97:77-86. Epub 1985/01/01. PubMed PMID: 2986247.
8. Houghton JA, Houghton PJ, Webber BL. Growth and characterization of childhood rhabdomyosarcomas as xenografts. Journal of the National Cancer Institute. 1982;68(3):437-43. Epub 1982/03/01. PubMed PMID: 6950170.
9. Herter-Sprie GS, Kung AL, Wong KK. New cast for a new era: preclinical cancer drug development revisited. The Journal of clinical investigation. 2013;123(9):3639-45. Epub 2013/09/04. doi: 10.1172/jci68340. PubMed PMID: 23999436; PubMed Central PMCID: PMCPMC3754257.
10. Hidalgo M, Amant F, Biankin AV, Budinska E, Byrne AT, Caldas C, et al. Patient-derived xenograft models: an emerging platform for translational cancer research. Cancer discovery. 2014;4(9):998-1013. Epub 2014/09/04. doi: 10.1158/2159-8290.cd-14-0001. PubMed PMID: 25185190; PubMed Central PMCID: PMCPMC4167608.
11. Teicher BA. Tumor models for efficacy determination. Molecular cancer therapeutics. 2006;5(10):2435-43. Epub 2006/10/17. doi: 10.1158/1535-7163.mct-06-0391. PubMed PMID: 17041086.
12. Tentler JJ, Tan AC, Weekes CD, Jimeno A, Leong S, Pitts TM, et al. Patient-derived tumour xenografts as models for oncology drug development. Nature reviews Clinical oncology. 2012;9(6):338-50. Epub 2012/04/18. doi: 10.1038/nrclinonc.2012.61. PubMed PMID: 22508028; PubMed Central PMCID: PMCPMC3928688.
13. Gambara G, Gaebler M, Keilholz U, Regenbrecht CRA, Silvestri A. From Chemotherapy to Combined Targeted Therapeutics: In Vitro and in Vivo Models to Decipher Intra-tumor Heterogeneity. Frontiers in pharmacology. 2018;9:77. Epub 2018/03/02. doi: 10.3389/fphar.2018.00077. PubMed PMID: 29491834; PubMed Central PMCID: PMCPMC5817069.
14. Dai W, Liu J, Li Q, Liu W, Li YX, Li YY. A comparison of next-generation sequencing analysis methods for cancer xenograft samples. Journal of genetics and genomics = Yi chuan xue bao. 2018;45(7):345-50. Epub 2018/07/30. doi: 10.1016/j.jgg.2018.07.001. PubMed PMID: 30055875.
15. Khandelwal G, Girotti MR, Smowton C, Taylor S, Wirth C, Dynowski M, et al. Next-Generation Sequencing Analysis and Algorithms for PDX and CDX Models. Molecular cancer research : MCR. 2017;15(8):1012-6. Epub 2017/04/27. doi: 10.1158/1541-7786.mcr-16-0431. PubMed PMID: 28442585.
16. Kluin RJC, Kemper K, Kuilman T, de Ruiter JR, Iyer V, Forment JV, et al. XenofilteR: computational deconvolution of mouse and human reads in tumor xenograft sequence data. BMC bioinformatics. 2018;19(1):366. Epub 2018/10/06. doi: 10.1186/s12859-018-2353-5. PubMed PMID: 30286710; PubMed Central PMCID: PMCPMC6172735.
17. Rossello FJ, Tothill RW, Britt K, Marini KD, Falzon J, Thomas DM, et al. Next-generation sequence analysis of cancer xenograft models. PloS one. 2013;8(9):e74432. Epub 2013/10/03. doi: 10.1371/journal.pone.0074432. PubMed PMID: 24086345; PubMed Central PMCID: PMCPMC3784448.
18. Collins AT, Lang SH. A systematic review of the validity of patient derived xenograft (PDX) models: the implications for translational research and personalised medicine. PeerJ. 2018;6:e5981. Epub 2018/12/01. doi: 10.7717/peerj.5981. PubMed PMID: 30498642; PubMed Central PMCID: PMCPMC6252062.
19. Gargiulo G. Next-Generation in vivo Modeling of Human Cancers. Frontiers in oncology. 2018;8:429. Epub 2018/10/27. doi: 10.3389/fonc.2018.00429. PubMed PMID: 30364119; PubMed Central PMCID: PMCPMC6192385.
20. Xu C, Li X, Liu P, Li M, Luo F. Patient-derived xenograft mouse models: A high fidelity tool for individualized medicine. Oncology letters. 2019;17(1):3-10. Epub 2019/01/19. doi: 10.3892/ol.2018.9583. PubMed PMID: 30655732; PubMed Central PMCID: PMCPMC6313209.
21. Hamburger AW, Salmon SE. Primary bioassay of human tumor stem cells. Science (New York, NY). 1977;197(4302):461-3. Epub 1977/07/29. PubMed PMID: 560061.